AD-A096 485 WASHINGTON UNIV SEATTLE POLAR SCIENCE CENTER F/G 17/9
SEA ICE DISPLACEMENT FROM SEASAT SYNTHETIC APERTURE RADAR,(U)
1981 R T HALL, D A ROTHROCK N00014-79-C-0418
UNCLASSIFIED NL

END
DATE FILMED
4-81
DTIC

SEA ICE DISPLACEMENT FROM SEASAT SYNTHETIC APERTURE RADAR

by

R. T. Hall and D. A. Rothrock

Polar Science Center
University of Washington

Contract N00014-79-C-0418

Submitted to Journal of Geophysical Research

1981

ABSTRACT

Images obtained by a synthetic aperture radar on SEASAT have been used to measure sea ice displacements over a three day interval in October 1978. The data points lie roughly along a line and are quite dense--about 2 km apart--over a distance of 863 km. The displacements are about twenty kilometers. Displacement errors grow with distance from shore becoming as large as 3 km. The graph of displacement versus distance has occasional discontinuities of several kilometers. Displacement discontinuities are accurate to ± 0.07 km along track and 3% of their magnitude across track.

INTRODUCTION

The motion of sea ice varies on all scales up to 10^3 km. The larger scale motions are driven by atmospheric pressure systems. On scales less than about 10^2 km the motion is affected by individual ice floes. The motion has traditionally been observed by tracking particles of ice: a couple of drifting manned camps, or a few buoys or radar reflectors. Each tracer is costly, limiting any experiment to on the order of ten points. Such methods do not reveal the spatial structure of the field of motion. What is needed are records thousands of kilometers long, sampled every kilometer or so.

Tracking natural ice features in satellite imagery improves the sampling rate. Following recognizable leads in LANDSAT visual photographs can provide records over 500 km long with about 25 irregularly spaced data points--an average spacing of 20 km [*Nye*, 1975]. Synthetic aperture radar (SAR) has the potential to provide yet more dense measurements. Its high resolution and sensitivity to surface roughness allow individual roughness features to be tracked, and these are more abundant than new leads.

The last decade has seen a considerable amount of radar imagery collected from aircraft. Airborne imaging radar data from 1975 was used to provide ice

displacements at spacings of about 10 km over an area roughly 10^4 km^2 [*Bryan et al.* 1977; *Leberl et al.* 1979]. But in general the distortion caused by the wide look angle and the aircraft motion discouraged quantitative analysis. It was not until generous amounts of quasi-corrected imagery from the L-band SAR on SEASAT became available through NOAA that the general sea ice community could experience firsthand the tantalizing potential of radar data.

This paper describes a technique for measuring ice displacements from these SAR images. It is not intended to be a comprehensive analysis of the performance of the system, but rather a report on some encouraging results. Measurements are presented of both components of displacement versus a single horizontal coordinate. This data record is 863 km long and has 417 data points--roughly one point every 2 km. Measurement errors are assessed by applying the same method to images of land where there are no displacements. The errors are discussed in terms of the satellite system and the optical data processing procedure. It appears that SEASAT SAR can provide 3 day displacements accurate to several kilometers and displacement discontinuities accurate to one or two hundred meters. With sufficient care, these errors could be reduced.

THE DATA

SEASAT operated from early July until 10 October 1978, collecting SAR data over swaths 100 km wide. More than 10^5 km of arctic data were collected, half of this over sea ice in the Beaufort, Chuckchi and East Siberian Seas south of 70°N. Often the sensor was turned on over North America, crossed the Arctic Ocean and was turned off over Siberia. Hence, there is often land at both ends of the swath which can be used both to eliminate some errors in the data and to assess those errors remaining.

The novel feature of SAR is that it combines data taken at different positions along the flight path to synthesize a radar image from an antenna much larger than actually used--thus providing the high resolution. [See, for example, *Harger*, 1970, or *Reeves*, 1975.] The data are transmitted from the satellite and stored in digital format. The synthesis of the bulk of this high resolution data is presently performed by the Jet Propulsion Laboratory in Pasadena by an optical rather than digital process. The 100 km swath is processed as four adjacent 25 km swaths. The scale is 1:500,000; hence, two millimeters on the film strip represent a distance of one kilometer. The resolution is about 0.035 km on the ground; 0.07 mm on the film. The film strips are 70 mm positive transparencies. Not all are of good quality; we received one strip with a systematic blurring and elongation of features and another with double images for each pixel. The technical details of the SEASAT SAR system are reviewed by *Jordan* [1980].

To measure displacement, one needs to know the position of a recognizable ice feature imaged from two successive orbits. Since there was no control on absolute location, we chose to use orbits three days apart (or a multiple of three) because these orbits are almost identical. We examined in detail orbits 1396, 1439, and 1482 on October 2, 5 and 8, knowing from NOAA VHRR images that there was ice movement during this period, and wanting the most winter-like ice conditions. The data reported here are drawn from the latter two orbits. The ground swath is shown in Figure 1. Furthermore, we looked only at features roughly in the center of a single 25 km swath, thus avoiding any need to register the adjacent film strips and also minimizing the effect of slant-range distortion.

MEASUREMENT TECHNIQUE

To identify features in two successive images, and to find their initial and subsequent positions in a common coordinate system, we have used a Bendix Analytical Plotter Model C. This machine normally functions as a stereographic mapping tool; we have used it as an x,y digitizer with the crucial feature that two images can be viewed simultaneously. A few guide lines are drawn on the images to help keep the viewer oriented as he searches for features. The two images are placed on the two viewing stages of the plotter, and the stages are independently moved until the two cursors are located on the same feature in both images. The x,y coordinates of the cursor positions relative to the viewing stages are then recorded. With this equipment, one can measure about twenty-five data points in an hour.

Since the Bendix plotter is designed to accept 24 cm x 24 cm aerial photographs, our long film strips had to be analyzed piecemeal in overlapping segments representing roughly 100 km of ground coverage. To reassemble the data from the segments into one long data record, two reference points were marked in the overlapped regions of each pair of adjacent segments and measured in both reference frames. Thus, the data from each segment could be translated into the reference frame of the previous segment, and the segments reassembled into one long record.

The coordinate system is defined by a combined use of time marks and land. The time marks are dots spaced along the edges of the film strip. They define both the inboard and outboard edge of the 25 km ground swath even though the imagery may extend a bit outside them. They would also define distance along track except for some glitch in the system. Our x-axis is taken to run through the inboard time marks on both images. The y-axis is perpendicular to x through the most westerly land feature on Banks Island.

We tried to find a measurable feature at least every 2 km in x. In some relatively featureless st. etches, this was difficult; in others, we could have found many data points in 2 km. Often one chooses a feature in one image but has difficulty finding its counterpart in the other image. There are two effects. In successive orbits, a moving object is viewed from different angles from which it has a different appearance to the radar. In addition, the ice features in question are at the limit of the resolution and are thus defined by a different grouping of pixels (picture elements) in successive images. Hence, a feature prominent in one image may be absent in the other or distorted enough to make one uncertain where the cursor should be placed. A somewhat lower magnification than the six power eyepiece in our Bendix plotter would actually help one identify features. On land, features were relatively easy to identify and measure, presumably because the land is stationary and we had chosen to look at nearly identical orbits. With the cursor on an ice feature in one image, our uncertainty in locating the feature in the other image is comparable to the resolution ± 35 m. This error pertains to positioning a bright return in the film image. There is still the question of how closely a bright feature seen in two images corresponds to one particular ice feature. We have not tested this, but the positioning error for ice features can only be greater than that for image features.

OBSERVED DISPLACEMENTS

The 25 km wide strips for the orbits we examined (Figure 1) include 460 km over the Canadian archipelago ($x < 0$) and 860 km of drifting ice between $x = 285$ and $x = 1148$ km. We made no measurements in the near shore region ($0 < x < 285$) where large displacements carried the ice to the extreme edge or completely out of the second image.

Ice displacements (u,v) from initial positions (x,y) are plotted in Figure 2 versus x only. The data disclose the motion of individual pieces of ice. Each piece has a solid body rotation and translation; between pieces are jumps in displacement. Figure 3 illustrates this by showing a line drawn from the first to the last point on each piece both before and after the displacement. We see rotations of several degrees, translations of ten to twenty-five kilometers, and displacement jumps up to several kilometers.

These data resolve the discontinuous nature of the field of motion, and they do so over a great enough distance to show many jumps. Thus we now have a data set from which to theorize about the structure of the ice displacement field and how the discontinuities in it change the ice cover. The opening and closing of leads, however, cannot be obtained directly from this one dimensional slice of a two dimensional displacement field. They require the component of a displacement jump normal to a line of discontinuity (or crack or lead), and we have not measured the directions of these lines. In fact, these directions are not well defined on the images.

Plots of the quantities shown in Figure 2 were made to the same scale as the image to see what correspondence there was between leads and displacement jumps. The leads of this October scene are not the meandering angular lines of April ice, but are more lacy like the open water surrounding summer floes. These lacy leads change shape and size with deformation. One might have expected the big events of deformation to occur where there was some striking lead-like feature, but this was generally not the case. At all large deformations we could see changes in leads, but the leads were usually modest (less than a kilometer)--not those that stood out for their size (2 to 4 km). Some areas which had many leads and looked ripe for deformation moved

rigidly. Areas which moved approximately rigidly but did show some relative displacement (several hundred meters)--like the noisy segment between x = 385 and x = 435 km--do in fact show many sites at which this deformation could have occurred. This sort of motion seems consistent with an autumn pack with many small floes being consolidated into a winter pack with larger pieces.

ERRORS

Our interest is in the accuracy of relative position (x,y), of displacement (u,v) and of displacement differences ($\Delta u, \Delta v$). We have

$$\begin{aligned} u &= x_a^2 - x_a^1 \\ v &= y_a^2 - y_a^1 \\ \Delta u &= (x_b^2 - x_b^1) - (x_a^2 - x_a^1) \\ \Delta v &= (y_b^2 - y_b^1) - (y_a^2 - y_a^1) \end{aligned} \tag{1}$$

where the subscript identifies the ice particle and the superscript, a time. Discontinuities in displacement occur for only a few unique pairs of adjacent particles.

Systematic errors arise from various sources which we will discuss in turn below. We cannot now eliminate these errors from the data; the discussion is aimed at eliminating them from future measurements of these SAR images. There is a random zero mean error due to the 35 m resolution of the system. Its standard deviation is 35 m in (x,y), $\sqrt{2}$ times this or 50 m in (u,v) and 70 m in ($\Delta u, \Delta v$). It is seen in Figure 4 as the vertical scatter about the trends.

Along track stretching. The mechanics of the processor can introduce stretching of up to 1% in the along track direction. We have compared our images to maps and find 0.25 to 0.50% stretching. Conservatively then, we take our values of x to have an error of 0.005 x.

When two images are compared, this stretching may add or partially cancel. We find that the image on October 8th is compressed about 0.26% relative to that on the 5th. This is the trend in Figure 4. Since this trend is not necessarily maintained out over the ice, we do not correct the data. If we had fixed land points in the Siberian end of our images, we would probably have enough information to remove or reduce this error. The resulting error in u is roughly -0.0026 x; at the far end of the strip (x = 1150 km) this amounts to 3 km. For displacement differences Δu, the errors in neighboring u's effectively cancel.

Across track drift. Figure 4 shows a nearly constant error in v of -0.0001 x +0.38 km. As with u, this error cancels when one calculates Δv for neighboring features. The error in v can arise from several effects, two related to the orbits and the third, to the processor. The two orbits are not quite identical but cross at a slight angle near their tops. This causes an apparent across track displacement which grows with distance from the crossing. The orbital data needed to remove this error are available. The other orbital contribution to this error is made by the practice of taking satellite altitude to be fixed when it actually is slowly changing along the orbit. Enough is known about the actual altitude to remove these errors. Occasionally (perhaps once or twice per orbit) the assumed altitude is corrected, and at these locations along the orbit, there is an apparent jump in the across track position. There were no altitude corrections in the images we studied. Different processor set ups can introduce an offset in the across track location of the orbit on the order of a few hundred meters. This can only be detected and removed by locating the x-axis with a land point as was done with the y-axis. Again land points at each end of the pass (in the absence of altitude corrections) would remove these sources of error.

Across track distortion. The relation between the slant range (the distance from the satellite to a point x,y on the ground) and the across track coordinate y is non-linear. For convenience it is approximated to be linear, introducing a distortion. The specification for the optically processed data is that this distortion be no more than 3% of the distance from the centerline of a 25 km strip. We have no independent check and so, use this value. The greatest distance from any of our data points to the centerline is 6.6 km, with an error of 0.2 km. The 3% systematic error in y causes a displacement error of 3% of v, and the error in Δv is 3% of Δv. It would be a simple matter to correct all y values for the across track error.

DISCUSSION

Despite some early pessimism about the quality of the SEASAT SAR optical data, from them one can obtain high quality measurements of ice movement. The major errors in our measurements can be removed with more work and information. One needs land in both ends of the ice imagery, orbital parameters (equatorial crossings), altitude data, and the correct relation between the across track coordinate and the slant range.

There is no handicap in working with images which have not been digitally corrected. Coordinates of features can be measured from the slightly distorted images and can be corrected by the same algorithms one would use to correct the whole image, with considerable saving in processing cost and effort. This statement may be as true for pattern recognition and area measurements as it is for displacement measurements. Others have made this point [e.g. *Leberl, et al.*, 1979], but we repeat it here for emphasis.

There are many ways to look at SAR data. Our approach has been limited to making observations along a line. Thus, we have avoided making mosaics and have minimized the problem of mapping different orbits into a common

coordinate system. Neither have we attempted to establish absolute position except for illustrating the orbit in Figure 1. Other researchers attempting a more general treatment will encounter more difficulties than we have. We are convinced though of the usefulness of these data and the pity of SEASAT's early failure.

There are more pairs of congruent strips of SAR data between July and October 1978. Their analysis could be expected to show some dramatic seasonal changes in the velocity field structure, both in the sizes of rigid pieces and in the variance of the motion. There does not seem to be enough data to explore regional differences.

Given that knowledge of ice motion is essential to any study of mass balance, high resolution radars are a promising source of data on an operational level. Their disadvantage is their high data rate. An alternative worth study is collecting radar data only in a small fraction of the polar oceans in data windows say 30 km in diameter spaced on a 500 km grid. The data set would serve the same purpose as an array of buoys. The details of the motion would not be observed operationally, but their statistics would be known from a few records of the sort reported here.

Acknowledgments. This work was supported by the Office of Naval Research (Contract N00014-79-C-0418). The staff of the Jet Propulsion Laboratory, Pasadena, freely assisted us by discussing the problems with the film data format and the satellite SAR system in general. In particular, we are grateful to Daniel Held, Brian Huneycutt, and Thomas Bicknell. Bruce Neednam at NOAA's Satellite Data Services Division deserves our thanks for his help in acquiring the particular images we wanted to use.

REFERENCES

Bryan L., T. Farr, F. Leberl and C. Elachi. Synthetic aperture radar imagery of the AIDJEX triangle. AIDJEX Bulletin No. 37, 161-166, +21 figures, 1977.

Harger, R. O. Synthetic Aperture Radar Systems. Academic Press, New York, 1970.

Jordan, R. L. The SEASAT-A synthetic aperture radar system. J. of Ocean Engineering, Vol. OE-5, No. 2, p. 154-164, 1980.

Leberl, F., M. L. Bryan, C. Elachi, T. Farr and W. Campbell. Mapping of sea ice and measurement of its drift using aircraft synthetic aperture radar images. J. Geophys. Res., 84, No. C4, p. 1827-1835, 1979.

Nye, J. F. The use of ERTS photographs to measure the movement and deformation of sea ice. J. Glaciol., 15, No. 73, p. 429-436, 1975.

Reeves, R. G., ed. Manual of Remote Sensing. Amer. Soc. of Photogrammetry, Fall Church, VA 22046, p. 454-466, 1975.

Figure Captions

Figure 1. Approximate ground path of the inboard SAR swath on 2, 5 and 8 October 1978. Solid lines outline the portion of the path where displacement measurements were made.

Figure 2. Sea ice displacements between 5 and 8 October 1978: (*upper*) along track displacement vs. along track position, (*lower*) across track displacement vs. along track position.

Figure 3. Motion of ice pieces from 5 to 8 October 1978. The line segments represent floes moving rigidly from the lower position to the upper position. For instance, the segment AB on 5 October moved to A'B' by 8 October.

Figure 4. Apparent displacement over land from 5 to 8 October 1978. Since the true displacement is zero, these data represent measurement errors.

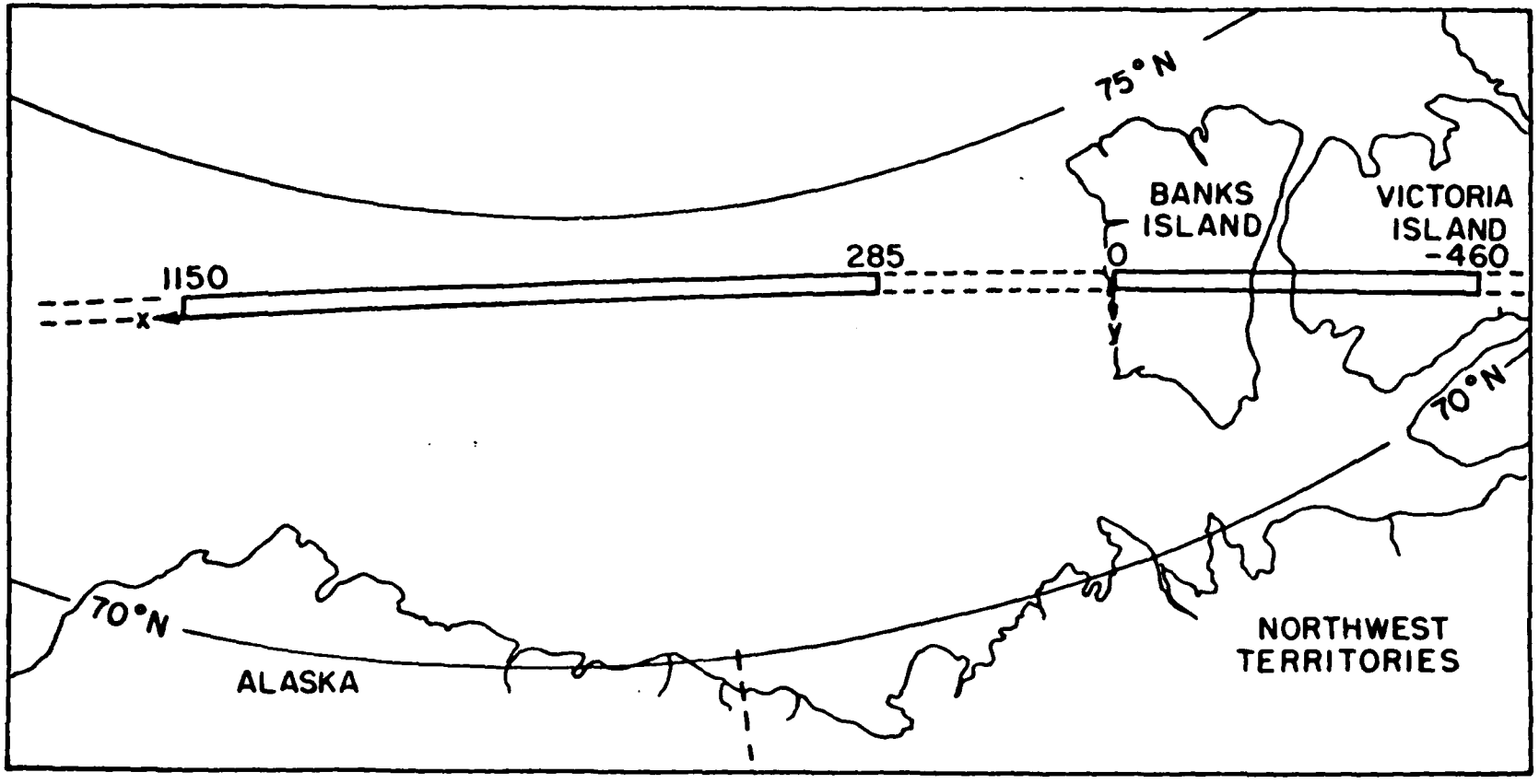

Fig. 1. Approximate ground path of the inboard SAR swath on 2, 5 and 8 October 1978. Solid lines outline the portion of the path where displacement measurements were made.

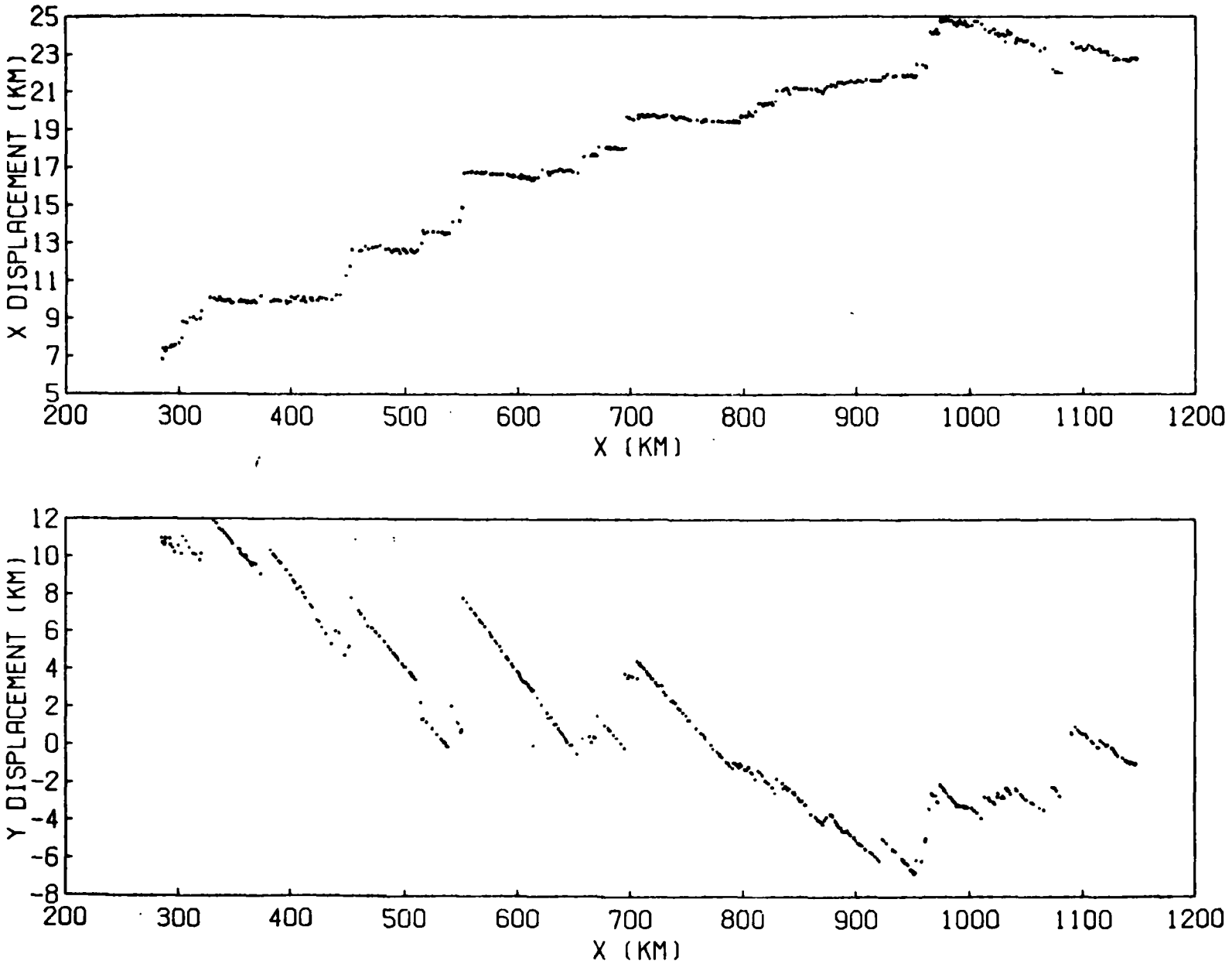

Fig. 2. Sea ice displacements between 5 and 8 October 1978: (*upper*) along track displacement vs. along track position, (*lower*) across track displacement vs. along track position.

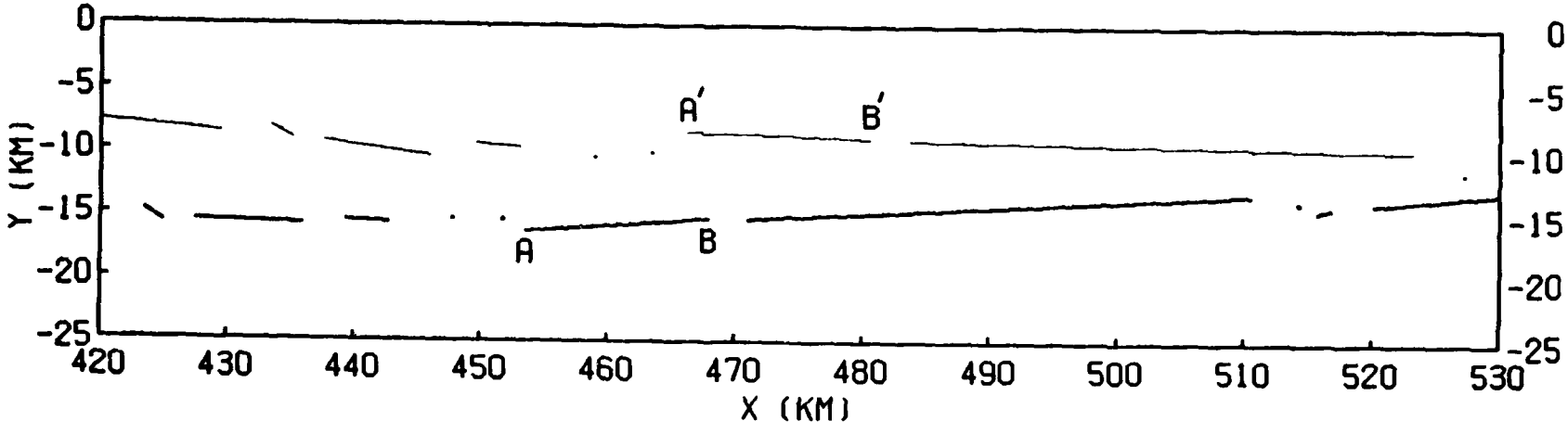

Fig. 3. Motion of ice pieces from 5 to 8 October 1978. The line segments represent floes moving rigidly from the lower position to the upper position. For instance, the segment AB on 5 October moved to A'B' by 8 October.

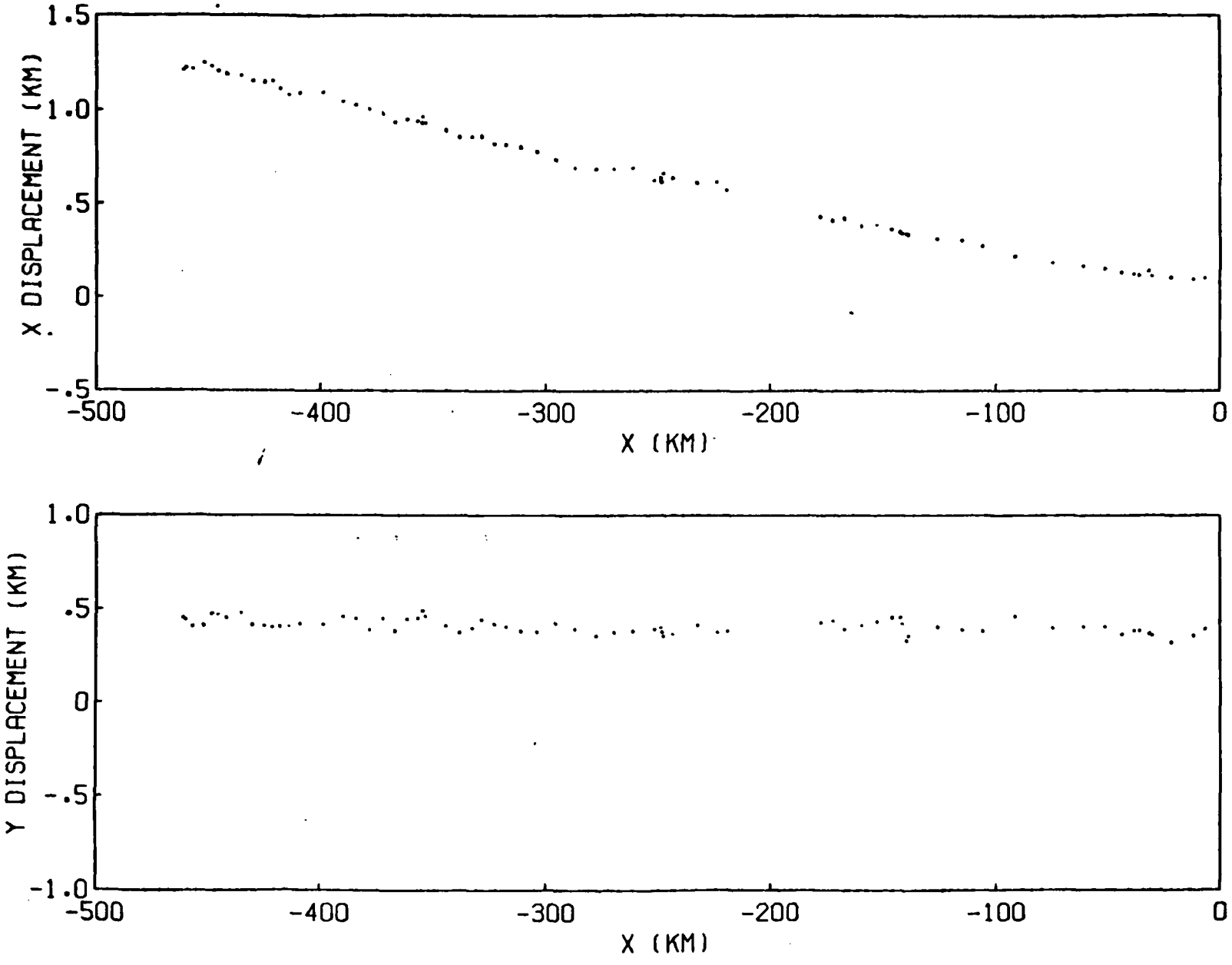

Fig. 4. Apparent displacement over land from 5 to 8 October 1978. Since the true displacement is zero, these data represent measurement errors.

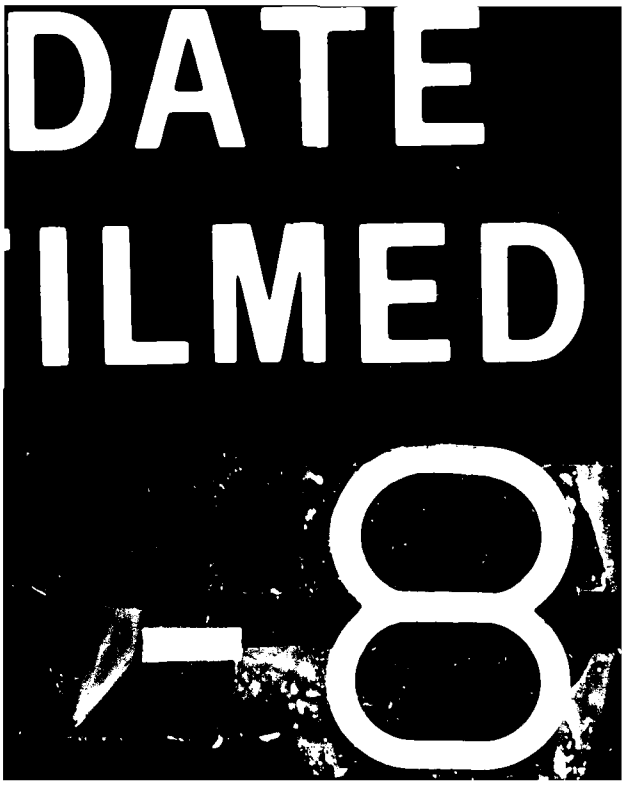
DATE
ILMED
-8